

## Article

# Analysis of the Ventilation Performance of a Solar Chimney Coupled to an Outdoor Wind and Indoor Heat Source

Shuaikun Yue <sup>1,†</sup>, Zhong Ge <sup>1,\*</sup>, Jian Xu <sup>1</sup>, Jianbin Xie <sup>1</sup>, Zhiyong Xie <sup>1</sup>, Songyuan Zhang <sup>2,†</sup> and Jian Li <sup>3,\*</sup> <sup>1</sup> School of Architecture and Urban Planning, Yunnan University, Kunming 650504, China<sup>2</sup> Faculty of Metallurgical and Mining, Kunming Metallurgy College, Kunming 650033, China<sup>3</sup> School of Mechanical Engineering, Beijing Institute of Technology, Beijing 100081, China

\* Correspondence: ynuzhongge@163.com (Z.G.); thulijian@163.com (J.L.)

† These authors contributed equally to this work.

**Abstract:** The effects of different solar radiation intensities, heat flow density of indoor heat sources, outdoor wind speed, and the relative location of indoor heat sources on the natural ventilation performance of solar chimneys are investigated through three-dimensional numerical simulations. The mechanism of the mutual coupling of the solar chimney effect with the outdoor wind and indoor heat source heat plume is explored. The results of the study show that when the structural parameters of the solar chimney are the same, the heat flow density on the surface of the indoor heat source, the outdoor wind speed and the solar radiation intensity all have a gaining effect on the ventilation performance of the solar chimney and the effects of the three on the ventilation of the solar chimney promote each other, when the solar radiation intensity is 200 W/m<sup>2</sup>, the outdoor wind speed is 1.0 m/s, and the indoor heat source heat flow density increases from 0 to 1500 W/m<sup>2</sup>, the solar chimney ventilation volume increases from 0.393 m<sup>3</sup>/s to 0.519 m<sup>3</sup>/s, the maximum value of the increase is 32.1%. In the other two cases, the maximum increase in solar chimney ventilation is 176.7% and 33.1%, respectively. Under the same conditions, solar chimney ventilation is optimal when the heat source is in the middle of the room. The presence of outdoor wind, however, affects the optimum design parameters of the solar chimney. Compared to the case where no outdoor wind is taken into account, the optimum inlet width of 0.2–0.3 m for the solar chimney no longer applies with outdoor wind, with the optimum value rising to 0.5 m.

**Keywords:** solar chimney; indoor heat source; natural ventilation; ventilation volume; solar radiation

**Citation:** Yue, S.; Ge, Z.; Xu, J.; Xie, J.; Xie, Z.; Zhang, S.; Li, J. Analysis of the Ventilation Performance of a Solar Chimney Coupled to an Outdoor Wind and Indoor Heat Source. *Appl. Sci.* **2023**, *13*, 2585. <https://doi.org/10.3390/app13042585>

Academic Editor: José António Correia

Received: 9 January 2023

Revised: 8 February 2023

Accepted: 10 February 2023

Published: 16 February 2023



**Copyright:** © 2023 by the authors. Licensee MDPI, Basel, Switzerland. This article is an open access article distributed under the terms and conditions of the Creative Commons Attribution (CC BY) license (<https://creativecommons.org/licenses/by/4.0/>).

## 1. Introduction

In recent years, energy consumption has been increasing, with buildings accounting for 20–40% of total energy consumption [1]. To reduce energy dependency and the impact of energy consumption, the development of “passive” energy buildings should be promoted [2]. Solar chimneys are attracting attention as a new, energy-efficient way to ventilate buildings. The use of solar chimneys will help to enhance ventilation [3,4], reduce energy consumption for building heating, ventilation, and air conditioning [5], save energy, and reduce building carbon emissions, among other things [6].

Solar energy is currently one of the most commonly used renewable energy sources. Solar chimneys use solar radiation to heat the air inside the chimney, providing buoyancy to the air and facilitating air flow through the chimney system. The simple structure of the solar chimney is mainly composed of a glass cover plate, heat collection wall, and air entrance and exit. To better promote indoor air flow, a combination of vertical and inclined solar chimneys is often used to increase the ability of the solar chimney to induce air [7–9].

The ventilation performance of a solar chimney is mainly influenced by its own structure and environmental conditions. Studies have shown that buildings with solar chimneys consume 10–20% less energy per day on average for air conditioning and can save

up to 30% in running costs compared to a normal room [10]. Li [11] takes a solar chimney in a warm temperate monsoon climate in Xi'an with an average summer temperature of 28 °C and a width-to-height ratio between 0.1 and 0.5 as the subject of his study and studied the induced air flow characteristics of air temperature distribution, wind speed distribution, and countercurrent phenomenon through experimental and theoretical analysis. The results show that the distribution of induced air temperature and air velocity is highly uneven, with an optimum chimney width-to-height ratio of 0.4. Mehran [12] studied the effect of different heights of solar chimneys with domed roofs and different inlet locations on the ventilation in the room, showing that the best overall ventilation performance of the passageway was achieved at a height of 0.7 m and an inlet in the lower part of the room. Dhahri [13] investigated the ventilation performance and thermal performance of four inlet shapes of vertical solar chimneys: horizontal, triangular, trapezoidal, and rounded angles by means of numerical simulations and showed that a solar chimney with a triangular inlet shape produces higher efficiency when used as a natural draft. He [14] investigated the enhancement of ventilation efficiency by inserting glass panels into the chimney channels to increase the thermal boundary layer by constructing an experimental model of a solar chimney 1.2 m high, 0.4 m wide, and 0.5 m deep. The results show that the insertion of plain glass panels in the chimney channel increases the chimney flow rate by 5% to 9% and that increasing the number of thermal boundary layers benefits the thermal efficiency of the chimney. Liu [15] carried out a numerical analysis of the ventilation performance of a combined tilted and vertical solar chimney and compared it with a vertical and tilted solar chimney to discuss the feasibility of different modes of operation and the effectiveness of ventilation under different environmental conditions. The results show that combined solar chimneys provide better ventilation than vertical and inclined solar chimneys and can avoid overheating problems. Leticia [16] conducted an experimental study of wind speed and direction on solar chimneys and found that the airflow rate at the exit of the solar chimney was mainly influenced by the outdoor wind speed and direction, with the volume flow rate at the exit of the chimney increasing significantly even at low speeds. Wang [17] investigated the effect of wind on the optimum design parameters for solar chimneys and showed that the optimum passage width rose from 0.2–0.3 m to 0.4–0.5 m. Gao [18] used numerical simulation to investigate the effects of channel width ratio and chimney inclination on the natural ventilation performance of a new rooftop solar chimney at different outdoor wind speeds. The results showed that the trend of the ventilation rate varied with the increase in passage width. The mass flow rate of the new structure increases with the increase in inclination angle. Shi [19] investigated numerically and theoretically the interaction between solar chimneys and outdoor winds and showed that higher wind speeds do not represent better ventilation performance, depending on the angle between the wind direction and the window, with solar chimneys exhibiting the best ventilation performance when the angle is 0.

The thermal buoyancy created by the difference in air density in a building can drive natural thermal pressure ventilation, an energy efficient ventilation method used to obtain higher air quality. Lin [20] investigated the effect of heat sources of different heights on the effect of natural ventilation driven by buoyancy forces by means of the scaled-down experimental water tank method and compared the experimental results with the theoretical calculations. The formulae for the effect of the model's effective inlet and outlet opening areas on the natural convection heat of the heat plume above the heat source were analyzed, and the area above the heat source was divided into a continuous plume zone, an interval plume zone, and a floating plume zone. Gao [21] investigated the interaction of heat plumes generated by two heat sources of the same intensity in a naturally ventilated space. The results show that when two heat sources are close to each other, the heat plumes from both come into contact immediately above the heat sources, and that the peak values of the velocity and temperature fields in the room do not change much with increasing the distance between the heat sources, while the room height remains constant. Barrios [22] analyzed the heat transfer and flow transition characteristics of the thermal plume generated by the

bottom-ground central heating element in a two-dimensional, rectangular enclosure when the Rayleigh number  $Ra$  was varied using thermal lattice-Boltzmann equation calculations.

From the available experimental and numerical simulation studies, it can be seen that the current research on solar chimneys focuses on the influence of structural and environmental parameters on their ventilation performance. In practice, in some buildings with high indoor heat sources such as substation rooms and data rooms, high indoor temperatures can affect the efficiency of machines and the thermal comfort of the human body when high-temperature heat sources are present in the room. In order to improve the indoor thermal environment, when using a solar chimney for natural ventilation, there is a solar chimney effect coupled with the outdoor wind and the heat plume of the indoor heat source. To address this problem, this paper establishes a three-dimensional numerical simulation of a solar chimney coupled with the outdoor wind field and indoor heat plume. analyzes the effects of outdoor wind speed  $V$ , indoor heat source heat flow density  $W$ , solar radiation intensity  $I$  and the relative position of the indoor heat source on the ventilation performance of the solar chimney. Provides a reference basis for the design, application, and optimization of solar chimney-induced ventilation in energy-efficient buildings.

## 2. Materials and Methods

### 2.1. Physical Model

This paper investigates the performance of solar chimney ventilation with the combined effects of solar radiation, outdoor wind field, and indoor heat source. A three-dimensional physical model of the system is shown in Figure 1. The solar chimney is located on the roof of the room and consists of an inclined section and a vertical section. The solar chimney is composed of the outer glass cover plates ACKI and EGYZ. The inner heat collection wall is composed of BDFH and JLYZ. And the middle air channel. The letters enclosing the area represent the meanings shown in Table 1. Its working principle is that part of the outdoor wind enters the room through the south window, and under the combined action of the solar radiation and the indoor heat source, the air enters the air passage through the lower entrance of the chimney. The heat collecting wall absorbs the solar radiation through the glass cover plate, so that the temperature of the air in the channel increases and the density decreases, forming the density difference between the external air and the external air, and accelerating the indoor air flow, discharging outdoors from the solar chimney channel. A part of the outdoor wind forms a negative pressure at the chimney outlet, forming a suction effect on the air inside the solar energy chimney. The structure improves indoor thermal comfort under the combined effect of thermal and wind pressure.

**Table 1.** The meaning of the letters enclosing the area.

Enclosed Area	Meaning
QRST, $Q_1R_1S_1T_1$	South window
UVWX, $U_1V_1W_1X_1$	North window
MNOP	Indoor heat source
ABCD, EFGH	Air inlet
IJKL	Air outlet
BDFH, JLYZ	Heat collecting walls
ACKI, EGYZ	Glass cover plate

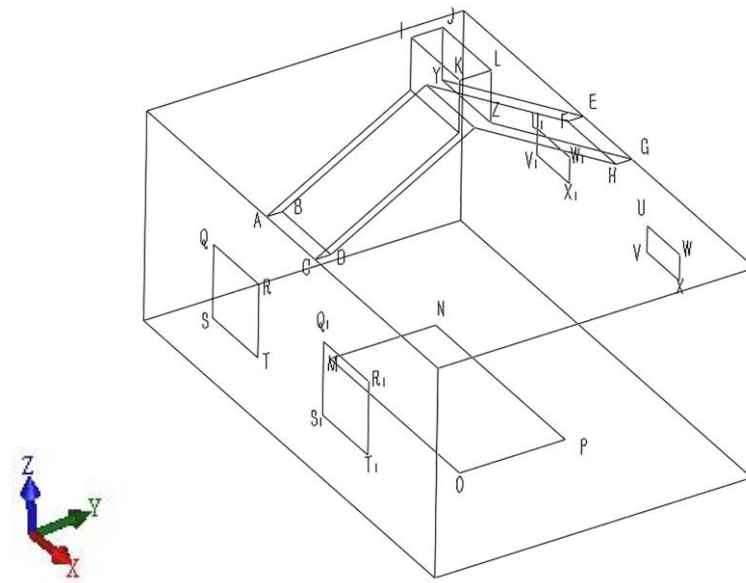


**Figure 1.** Physical model of solar chimney building.

## 2.2. Calculation Area

The calculation area for the solar chimney building is shown in Figure 2. The geometry of the room is  $9000 \times 6000 \times 4000$  mm. The geometry of the indoor heat source is  $4000 \times 2000$  mm and is located in the center of the room. The south wall of the room is provided with two  $1400 \times 1400$  mm windows QRST,  $Q_1R_1S_1T_1$ . Spaced at 3400 mm centers, with their lower edges 1200 mm from the floor. The north wall of the room is provided with UVWX,  $U_1V_1W_1X_1$  two windows of  $1000 \times 500$  mm with a center spacing of 3400 mm and their lower edge at 2500 mm from the floor. ABCD and EFGH are the inlet of the chimney with a geometry of  $1500 \times 300$  mm. IJKL is the outlet of the chimney, with a geometry of  $1500 \times 600$  mm. The angle between the inclined chimney section and the horizontal direction is  $30^\circ$ , and the height of the vertical chimney section LZ is 1000 mm. The size of the numerical simulation calculation domain is determined according to the building guidelines. The side and top boundaries are 18, 18, and 30 m from the building, respectively. Wind speed inlet  $A_1B_1C_1D_1$  is 30 m from the building, and in order for the building's wake to fully develop, wind speed outlet  $E_1F_1G_1H_1$  is 60 m from the building.

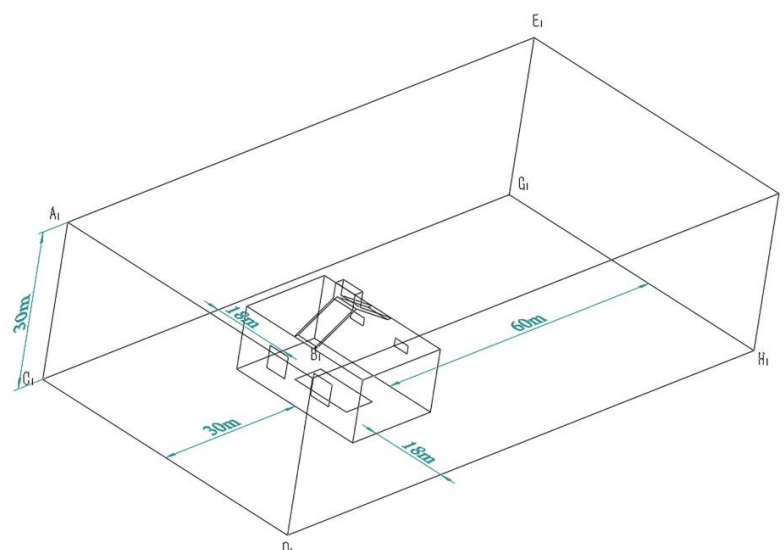


**Figure 2.** Outdoor wind field boundary of solar chimney building.

### 2.3. Mathematical Models

Numerical simulations of the above model were carried out using Fluent software. The theoretical equations for three-dimensional steady-state turbulent flow [23] are as follows.

The continuity equation is:

$$\frac{\partial u_i}{\partial x_i} = 0 \tag{1}$$

The momentum equation is:

$$\frac{\partial(u_i u_j)}{\partial x_j} = -\frac{1}{\rho} \frac{\partial P}{\partial x_i} + \frac{\partial}{\partial x_j} \left[ (v + v_t) \frac{\partial u_i}{\partial x_j} \right] - \beta g_i (T - T_\infty) \tag{2}$$

$\beta g_i (T - T_\infty)$  derived from fluid density variations, obtained from the Boussinesq hypothesis term. The hypothesis considers the entire system to be non-pressurized flow, except for the buoyancy force term in vertical flow.

The energy equation is:

$$\frac{\partial(u_i T)}{\partial x_j} = \frac{\partial}{\partial x_j} \left[ \Gamma \frac{\partial u_i}{\partial x_j} \right] \tag{3}$$

The heat transfer process in a combined solar chimney is a complex, dynamic process involving thermal convection and radiation. In order to simplify the theoretical analysis and numerical calculations, the fluid is assumed to flow fully turbulently and to reduce calculation errors where the enhanced wall function method is used near the walls. To simplify the heat transfer process, air infiltration and heat storage on the chimney walls are neglected. The turbulent kinetic energy ( $k$ ) and the corresponding dissipation rate ( $\epsilon$ ) can be determined as [24]:

$$\frac{\partial(k u_i)}{\partial x_i} = \frac{1}{\rho} \frac{\partial}{\partial x_j} \left[ \left( v + \frac{v_t}{\sigma_k} \right) \frac{\partial k}{\partial x_j} \right] + G_k - \epsilon \tag{4}$$

$$\frac{\partial(\epsilon u_i)}{\partial x_i} = \frac{1}{\rho} \frac{\partial}{\partial x_j} \left[ \left( v + \frac{v_t}{\sigma_\epsilon} \right) \frac{\partial \epsilon}{\partial x_j} \right] + \frac{\epsilon}{k} (c_1 G_k - c_2 \epsilon) \tag{5}$$

$$G_k = \frac{v_t}{\rho} \frac{\partial u_i}{\partial x_j} \left( \frac{\partial u_i}{\partial x_j} + \frac{\partial u_j}{\partial x_i} \right) \tag{6}$$

where:  $x_i$  is the coordinate value, m;  $u_i$  is the mean velocity component in the  $x_i$  direction, m/s;  $\rho$  is the density of air, kg/m<sup>3</sup>;  $P$  is the difference between pressure and ambient pressure, Pa;  $v_t, v$  is the coefficient of viscosity for turbulent and laminar flows, m<sup>2</sup>/s;  $g_i$  is the acceleration of gravity in the vertical direction, taken as 9.8 m/s<sup>2</sup>;  $\beta$  is the coefficient of thermal expansion of air, 1/K;  $T, T_\infty$  is the average temperature and the reference point temperature, K;  $\Gamma$  is the generalized diffusion coefficient;  $k$  is turbulent kinetic energy;  $\epsilon$  is the rate of dissipation of turbulent kinetic energy;  $c_1, c_2$  is an empirical factor;  $G_k$  is the turbulent kinetic energy generation term;  $p_r$  is the Prandtl number;  $\sigma_k, \sigma_\epsilon, \sigma_t$  take the standard experimental values.

### 2.4. Boundary Conditions

The air flowing in the model is based on the Boussinesq hypothesis dealing with the buoyancy term in the momentum equation; the model is solved using the finite volume method; and the coupling between velocity and pressure in the model is performed using the SIMPLE algorithm; the numerical model is an RNG  $k$ –epsilon two equation model with a discrete convective term in second order windward format; the DO radiation model can be applied to radiation problems in all optical depth ranges and can also solve radiation problems involving media. As this paper investigates the presence of heat sources within

the room, the DO radiation model is introduced to address both wall radiation and radiation involving gases, where the heat flow density of a heat source is expressed as the amount of heat passing through an object per unit cross-sectional area per unit time. The solar radiation intensity is set to be constant, the heat absorption and transmittance of the glass and collector panels are also kept constant, and the heat flux values of the glass and collector panels can be calculated from the solar radiation intensity and the physical properties of the material parameters. Slip-free conditions are used for all solid wall velocities with an outdoor temperature of 300 K. The atmospheric pressure is 101,325 Pa.

As shown in Figures 1 and 2: Plane  $A_1B_1C_1D_1$  is the velocity inlet. An exponential wind profile is selected as the inlet boundary condition, the terrain category is selected as class 2, and the exponential law  $\alpha$  is 0.22. The wind speed at the inlet reference of the calculation domain varies according to six levels from 0.5 to 3 m/s, and the simulated ambient temperature is set at 300 K. The velocity direction is parallel to the xy plane; plane  $E_1F_1G_1H_1$  is the pressure outlet; its relative total pressure is set to zero; the planes  $A_1C_1E_1G_1$ ,  $A_1B_1E_1F_1$  and  $B_1D_1F_1H_1$  are symmetrical surfaces; plane  $C_1D_1G_1H_1$  is the ground; the room walls are wall conditions, and their inner surfaces are subject to radiant heat exchange with the indoor heat source. The specific physical parameters of the relevant materials are shown in Table 2.

**Table 2.** Physical parameters of the main materials and air.

Material	Thickness	Density	Heat Conductivity Coefficient	Specific Heat Capacity	Solar Radiation		
	mm	kg/m <sup>3</sup>	W/(m·k)	J/(kg·k)	Transmittance	Reflectance	Absorption Rate
Glass cover plate	3	2500	0.75	837.4	0.84	0.1	0.06
Polyvinyl chloride	50	100	0.047	1380	0	0.05	0.95
Air	—	1.205	0.0259	1005.43	1	0	0
Insulated walls	200	1800	0.814	879	0	1	0

### 3. Validation

#### 3.1. Mesh Independence Verification

The calculations are complicated by the presence of outdoor wind fields and solar chimneys in the calculation area. Structured and unstructured grids are used to divide the model. To ensure the accuracy of the calculation results a grid encryption is used near the heat source and the chimney channel. The local encryption calculation grid is shown in Figure 3. The grid independence is assessed during the calculation and simulation to generate six sets of grids, the grid numbers are 842,790, 963,847, 1,056,646, 1,188,238, 1,318,472, and 1,408,494, and the values of natural ventilation under different grids are shown in Figure 4. The deviation between the ventilation values of the 4th and 5th grids is only 1%, and the 4th grid is chosen for the numerical simulation due to the accuracy of the results and the speed of calculation.

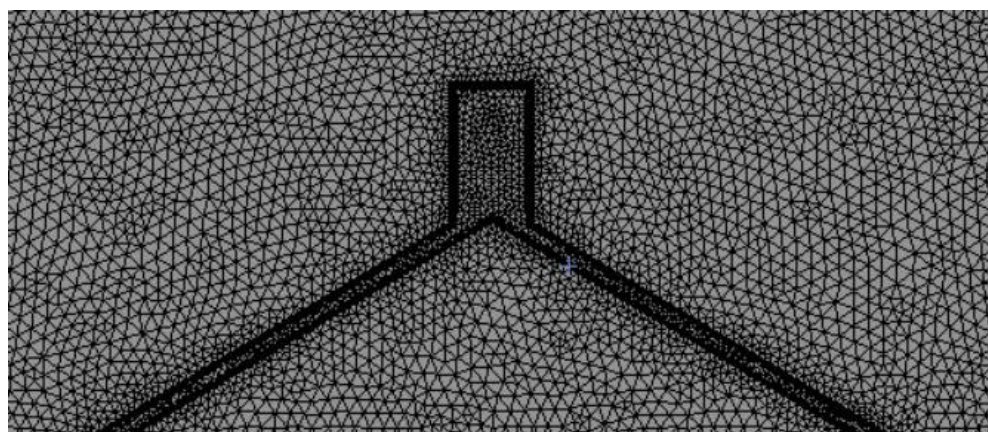


**Figure 3.** Grid independence assessment.

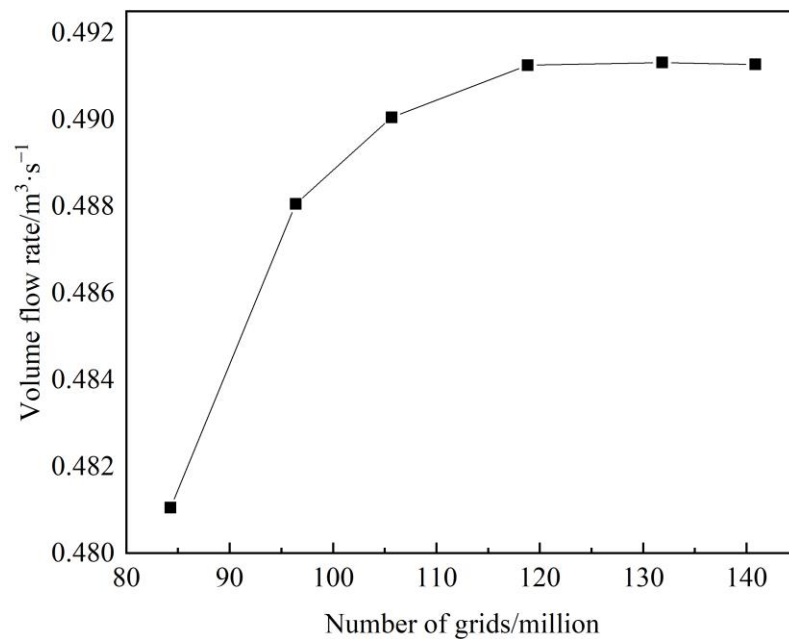


**Figure 4.** Local grid densification of solar chimney.

### 3.2. Model Validation

To verify the feasibility of the method used in this paper, numerical simulations of solar chimney-induced draught under the experimental conditions of the literature [11] were carried out, and a comparison of the simulation results with the experimental results is shown in Figure 5. Under experimental conditions, a solar chimney (height 2000 mm, width 1000 mm, and depth 200–1000 mm, taken as 600 mm) was formed by a collector plate, a glass plate, and two side panels, using the electric heating method instead of the radiation value of the sun, with heat fluxes of 100–600  $\text{W}/\text{m}^2$ . The results show that the solar chimney-induced ventilation increases as the heat flux increases, which is in good agreement with the results from the experiments, and that the experimental data are within 8% of the simulated results, which is within the permissible margin of error. This is a good indication of the reliability of the model and calculation method used in this paper.

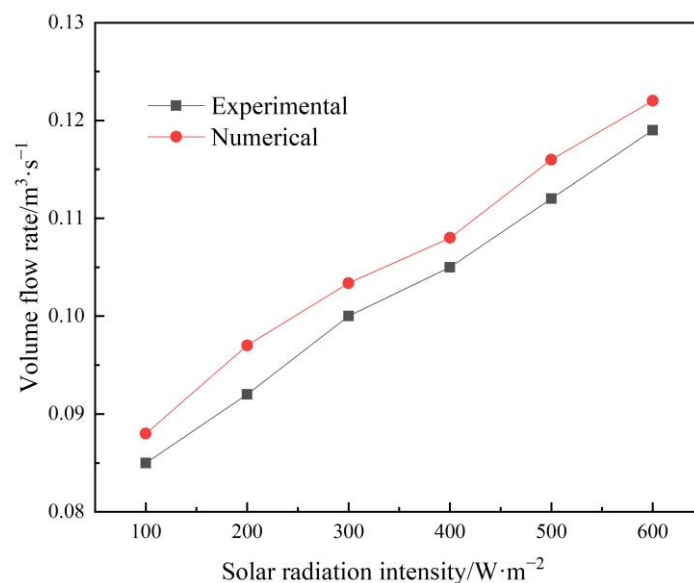
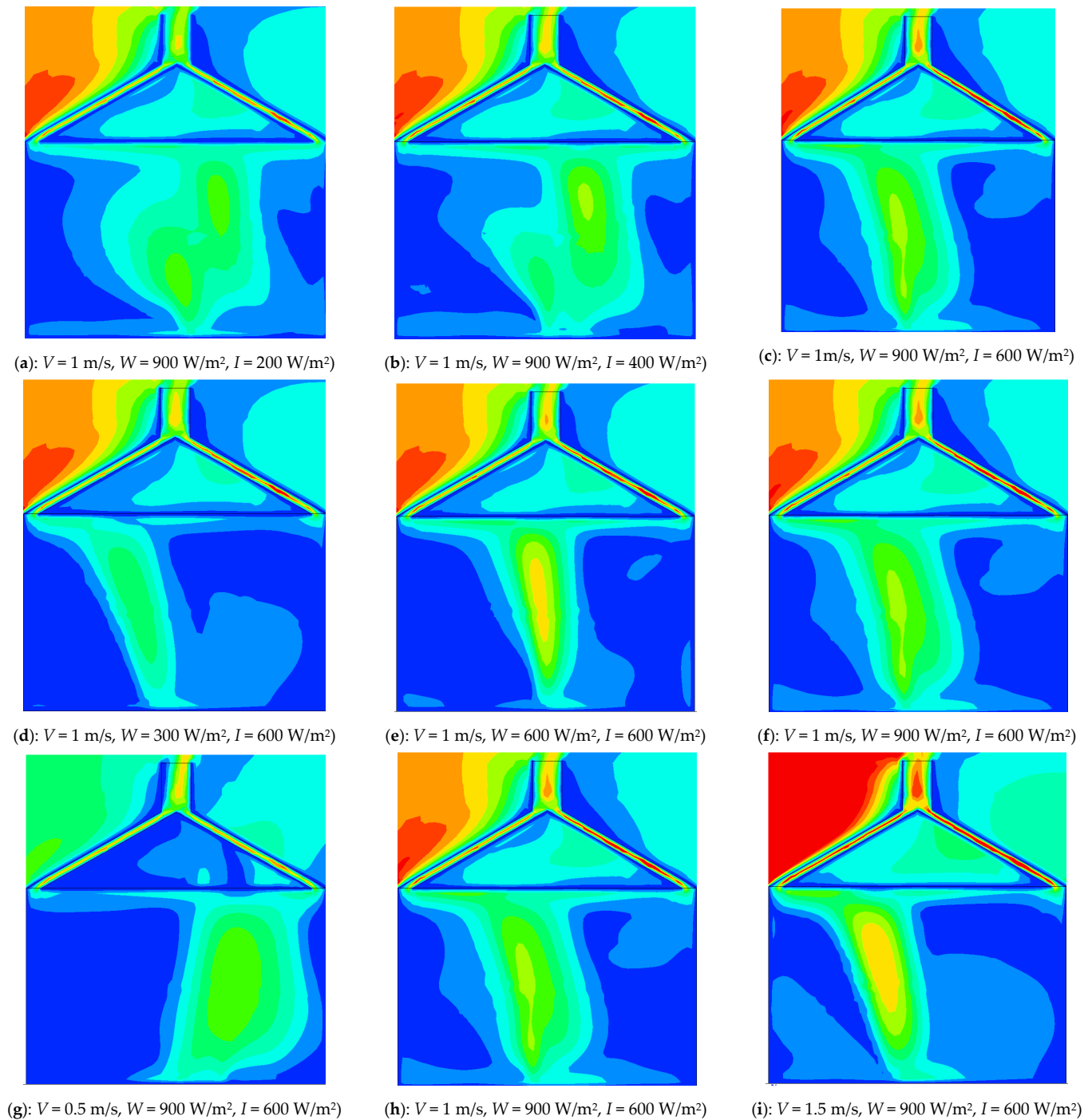


**Figure 5.** Comparison of experimental data [11] and simulated data.

## 4. Results and Discussion

### 4.1. Indoor Air Velocity Distribution at $X = 4.5$ m

The air velocity distribution inside the solar chimney building at  $X = 4.5$  m is shown in Figure 6, where  $W$  is the heat flow density of the internal heat source;  $V$  is the outdoor wind speed;  $I$  is the solar radiation intensity; and the geometry of the internal heat source is  $4000 \times 2000$  mm.



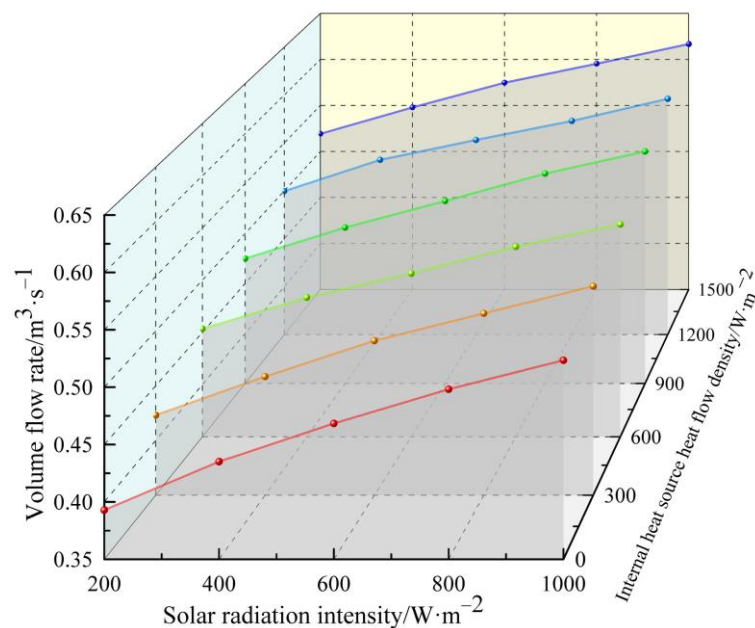
**Figure 6.** Indoor air velocity distribution at  $X = 4.5$  m.

Figure 6a–c shows the cloud diagram of indoor wind speed change from  $200$  W/m<sup>2</sup> to  $600$  W/m<sup>2</sup> when the outdoor wind speed and the heat flow density of the internal heat source are certain. From the diagram, it can be seen that as the solar radiation intensity

increases, the area of the indoor high wind speed zone becomes smaller and smaller, but the central speed will gradually increase. This is due to the fact that as the solar radiation intensity increases, the solar chimney's ability to draw air into the room increases the velocity of air flow in the room. The average velocity of the solar chimney outlet increased from 0.569 to 0.644 m/s, an increase of 13.2%. From the d-e indoor air velocity variation clouds, it can be seen that as the density of heat flow from the indoor heat source increases, the intensity of the heat plume at the surface of the heat source also increases, strengthening the ability to exchange heat with the indoor air, resulting in a gradual increase in the area of the high air velocity zone in the room. Figure 6g–i shows a cloud plot of the indoor wind speed variation as the outdoor wind speed changes from 0.5 to 1.5 m/s. It can be seen that the area of the indoor high wind speed zone gradually decreases, but the velocity increase in the central area is greater, and the velocity inside the solar chimney changes faster. The average velocity at the exit of the solar chimney increases from 0.605 to 0.755 m/s, an increase of 24.8%.

#### 4.2. Variation of Ventilation Volume with Solar Radiation Intensity

Figure 7 shows the variation curve of solar chimney ventilation with solar radiation intensity at different internal heat source heat flow densities, where: internal heat source heat flow density  $W$  is 0–1500  $W/m^2$ ; solar radiation intensity  $I$  is 200–1000  $W/m^2$ ; internal heat source geometry size is  $4000 \times 2000$  mm.



Different heat flow densities from internal heat sources ( $V = 1$  m/s).

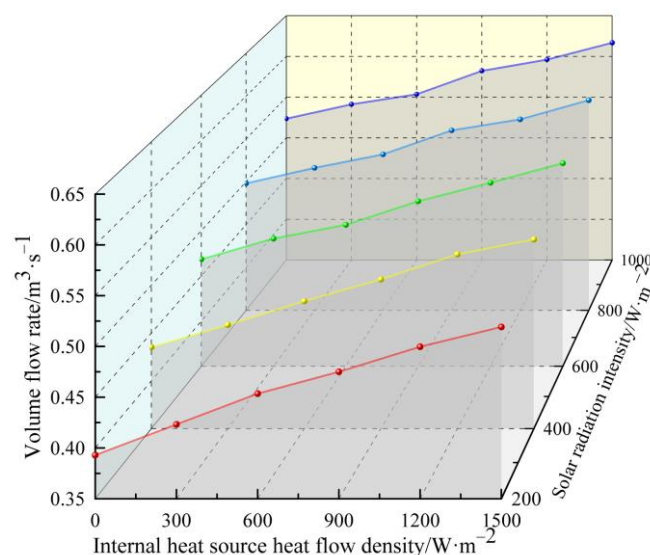
**Figure 7.** Variation of ventilation volume with solar radiation intensity.

As can be seen from Figure 7, when the outdoor wind speed is 1 m/s, the trend of the ventilation in the solar chimney is approximately the same for different heat flow densities of the internal heat source. As the intensity of solar radiation increases, the amount of ventilation in the solar chimney also increases. When the solar radiation intensity increases from 200 to 1000  $W/m^2$  and the heat flow density of the indoor heat source is 0, the solar chimney ventilation increases from 0.393 to 0.523  $m^3/s$ , a relative increase of 33.1% in ventilation; with a heat flow density of 1500  $W/m^2$  from the indoor heat source, the solar chimney ventilation volume increases from 0.519 to 0.617  $m^3/s$ , a relative increase of 18.9% in ventilation. The results show that the effect of solar radiation intensity on ventilation is diminished as the heat flow density of the indoor heat source increases. In buildings with solar chimneys and internal high-temperature heat sources, the solar

chimney and the heat source have a coupling effect on natural ventilation. As the intensity of solar radiation increases, the heat collecting wall absorbs more heat, which increases the heat gain of the air in the chimney channel. The temperature rises, the density difference increases, and the airflow float driving force generated by the density difference gradually increases, which in turn leads to an increase in ventilation. With the gradual increase in the density of heat flow from the indoor heat source, the heat plume generated on the surface of the heat source and the indoor air undergo natural convective heat exchange, increasing the impact of the buoyant heat plume on ventilation, increasing the impact of the internal heat source on natural ventilation, and relatively decreasing the impact of solar radiation intensity on ventilation.

#### 4.3. Change of Ventilation Rate with Heat Flux of Indoor Heat Source

Figure 8 shows the variation of solar chimney ventilation with the heat flow density of the indoor heat source under different solar radiation intensities. As can be seen from Figure 8, when the outdoor wind speed is 1 m/s, the solar chimney ventilation volume shows an increasing trend with the increase in the heat flow density of the indoor heat source. However, the increase in ventilation volume tends to decrease with the increase in solar radiation intensity. When the indoor heat source heat flow density increases from 0 to 1500 W/m<sup>2</sup> and the solar radiation intensity is 200 W/m<sup>2</sup>, the solar chimney ventilation volume increases from 0.393 to 0.519 m<sup>3</sup>/s, with a relative increase of 32.1%; when the solar radiation intensity is 1000 W/m<sup>2</sup>, the solar chimney ventilation volume increases by 17.8%. The results show that when the density of heat flow from the indoor heat source increases, the intensity of the heat plume at the surface of the heat source also increases, enhancing the ability to exchange heat with the indoor air, resulting in more air flowing into the solar chimney and increasing its ventilation capacity. When the intensity of solar radiation increases, the air in the chimney absorbs more heat, resulting in higher temperatures, and the increased density difference increases the rate of upward outflow of airflow, weakening the effect of the density of heat flow from the indoor heat source on the ventilation volume. The presence of an indoor heat source increases the ventilation capacity of a solar chimney compared to considering only the effect of solar radiation intensity on the ventilation effectiveness of a solar chimney.

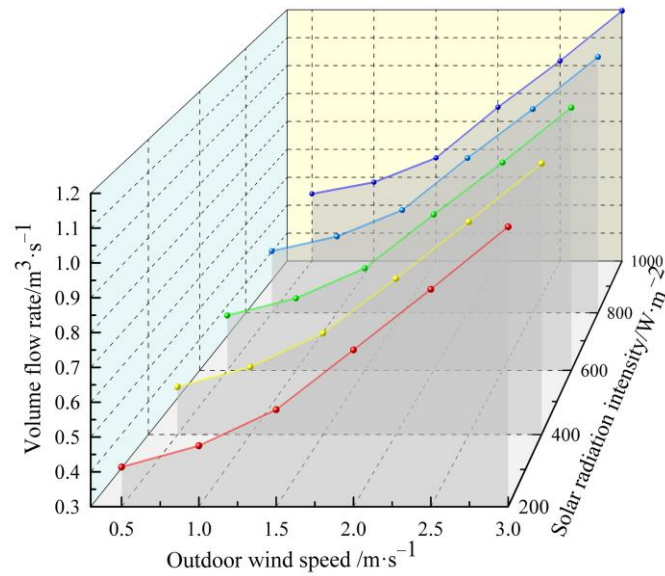


Different solar radiation intensity ( $V = 1$  m/s)

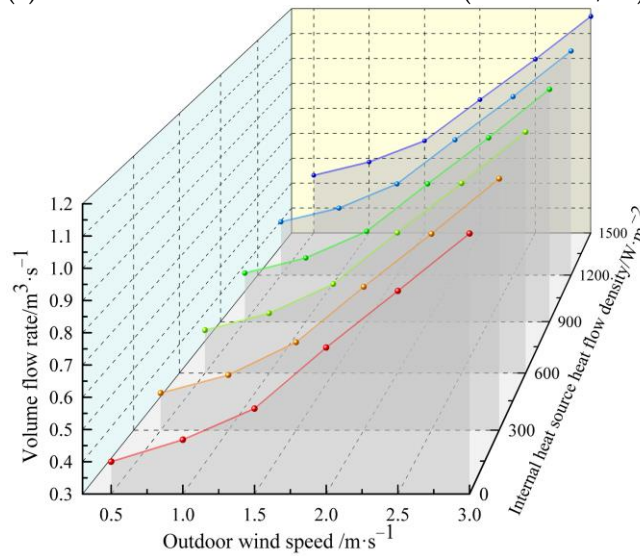
**Figure 8.** Change of ventilation rate with heat flux of indoor heat source.

4.4. Change of Ventilation Volume with Outdoor Wind Speed

Figure 9a,b shows the variation curves of solar chimney ventilation with outdoor wind speed  $V$  for different solar radiation intensities and heat flow densities of indoor heat sources. The outdoor wind speed is taken to be 0.5 to 3.0 m/s.



(a) Different solar radiation intensities ( $W = 900 \text{ W/m}^2$ )



(b) Different heat flow densities from internal heat sources ( $I = 600 \text{ W/m}^2$ )

**Figure 9.** Change of ventilation volume with outdoor wind speed.

As can be seen from Figure 9a, the trend of solar chimney ventilation is approximately the same for different solar radiation intensities at an indoor heat source heat flow density  $W$  of  $900 \text{ W/m}^2$ . As the outdoor wind speed increases, the chimney ventilation volume also increases, and by a large margin. At a solar radiation intensity of  $200 \text{ W/m}^2$ , as the outdoor wind speed  $V$  increases from 0.5 to 3 m/s, the solar chimney ventilation volume increases from  $0.414$  to  $1.104 \text{ m}^3/\text{s}$ , a relative increase of 166.7%; at a solar radiation intensity  $I$  of  $1000 \text{ W/m}^2$ , the ventilation volume increases by 121.1%.

As can be seen from Figure 9b, at different heat flow densities of the internal heat source, the ventilation of the solar chimney increases with increasing outdoor wind speed, but the increase decreases with increasing heat flow density of the indoor heat source. With an indoor heat source heat flow density  $W$  of 0, as the outdoor wind speed  $V$  increases

from 0.5 m/s to 3 m/s, the solar chimney ventilation increases from 0.400 to 1.108 m<sup>3</sup>/s, a relative increase of 176.7%; with an indoor heat source heat flow density  $W$  of 1 500 W/m<sup>2</sup>, the solar chimney ventilation increases by 120.1%. When part of the outdoor wind enters the room from the window, with the increase in wind speed, it will intensify the convective disturbance with the thermal buoyancy plume of the internal heat source. Part of the outdoor wind at the chimney outlet, with the increase in wind speed, will improve the extraction capacity of the chimney, the wind becomes the dominant factor in the ventilation of the solar chimney, weakening the influence of the indoor heat source on the ventilation of the chimney. The presence of wind pressure significantly enhances the ventilation capacity of a solar chimney compared to considering only the effect of thermal pressure on the ventilation effectiveness of a solar chimney.

4.5. Variation of Ventilation with the Position of the Internal Heat Source

Figure 10 shows the indoor heat source located within a north-west-oriented building schematic, with a geometry of 4000 × 2000 mm and a distance of 100 mm from the adjacent wall face, respectively. Figure 11 shows the variation of solar chimney ventilation versus indoor heat source location for different solar radiation intensities, indoor heat source heat flow density, and outdoor wind speed.

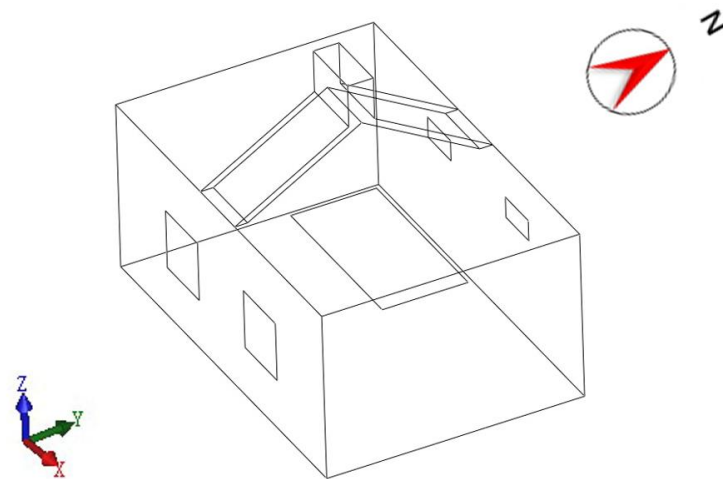
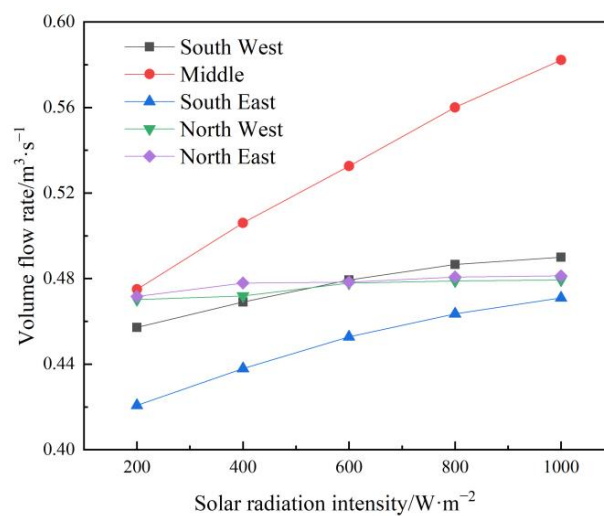
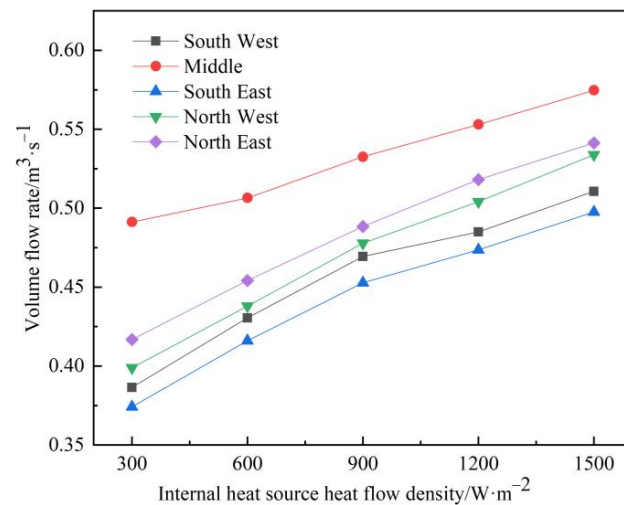
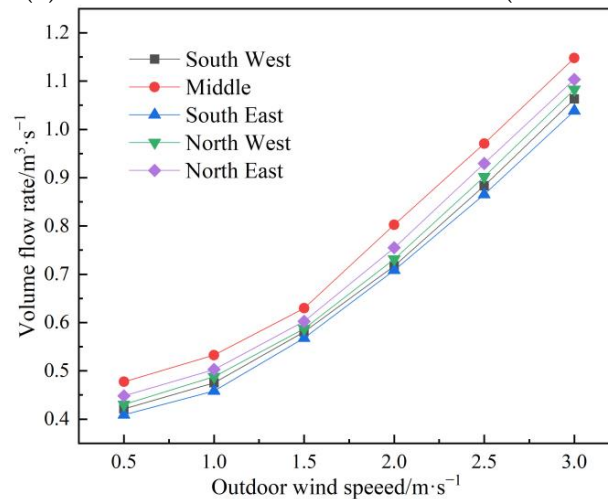


Figure 10. Model of building with heat source to the northwest.



(a) Different internal heat source locations ( $W = 900 \text{ W/m}^2$ ,  $V = 1.0 \text{ m/s}$ )

Figure 11. Cont.

(b) Different internal heat source locations ( $I = 600 \text{ W/m}^2$ ,  $V = 1.0 \text{ m/s}$ )(c) Different internal heat source locations ( $I = 600 \text{ W/m}^2$ ,  $W = 900 \text{ W/m}^2$ )**Figure 11.** Variation of ventilation with the position of the internal heat source.

As can be seen from Figure 11a, when the internal heat source  $W = 900 \text{ W/m}^2$  and the outdoor wind speed  $V = 1.0 \text{ m/s}$ , the solar chimney ventilation volume increases with the increase in solar radiation intensity for the heat sources located in the southwest, southeast, and middle directions, with increases of 7.2, 11.9, and 22.6%, respectively. When the heat source is located in the northwest and northeast, the solar chimney ventilation volume does not change much as the solar radiation intensity increases.

As can be seen from Figure 11b, when the solar radiation intensity  $I = 600 \text{ W/m}^2$  and the outdoor wind speed  $V = 1.0 \text{ m/s}$ , the solar chimney ventilation increases with the increase in the heat flow density of the indoor heat source, and the solar chimney ventilation effect reaches its best state when the heat source is in the middle of the room. As the heat flow density of the indoor heat source gradually increases from 300 to 1500  $\text{W/m}^2$ , the solar chimney ventilation increases from 0.491 to 0.575  $\text{m}^3/\text{s}$ , a relative increase of 17.1% in ventilation volume. Heat sources in the south-east and south-west locations are significantly less effective in venting their solar chimneys than those in the north-east and north-west locations, as the former are more disturbed by outdoor wind speeds than the latter.

As can be seen from Figure 11c, when the solar radiation intensity  $I = 600 \text{ W/m}^2$  and the heat flow density of the indoor heat source  $W = 900 \text{ W/m}^2$ , the solar chimney ventilation volume increases with the increase in outdoor wind speed, and the increase is larger. When the outdoor wind speed is 3.0  $\text{m/s}$  and the heat source is in the middle of the room, the maximum solar chimney ventilation volume reaches 1.14  $\text{m}^3/\text{s}$ .

#### 4.6. Variation of Ventilation Volume with Solar Chimney Inlet Width

Figure 12 shows the variation of the solar chimney ventilation versus the solar chimney inlet width at different outdoor wind speeds, where: the heat flow density  $W$  of the internal heat source is  $900 \text{ W/m}^2$ ; the solar radiation intensity  $I$  is  $600 \text{ W/m}^2$ ; and the geometry of the internal heat source is  $4000 \times 2000 \text{ mm}$ .

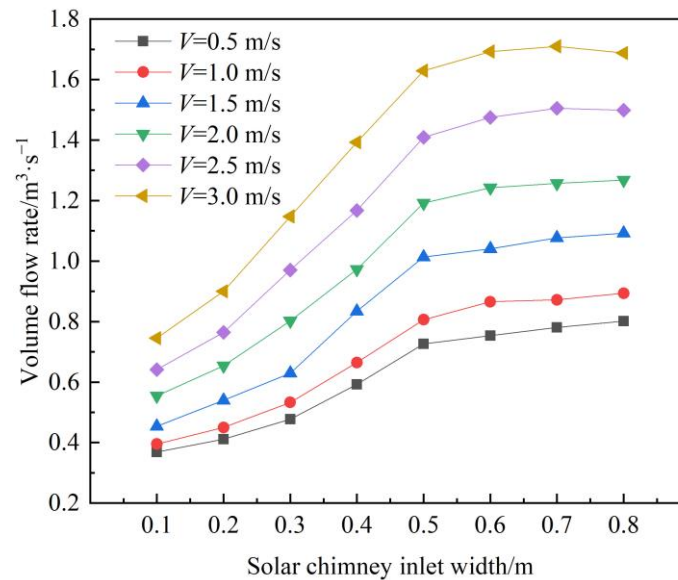


**Figure 12.** Variation of ventilation volume with solar chimney inlet width.

As can be seen from Figure 12, the ventilation of solar chimneys does not always increase with increasing inlet width, and when the inlet width is greater than 0.5 m, the trend of increasing ventilation does not increase significantly or even decreases. When the inlet width is less than 0.5 m, the ventilation volume increases significantly with increasing inlet width. For example, when the external wind speed is 1 m/s and the inlet width is increased from 0.1 to 0.5 m, the increase in ventilation volume is 104.1%. However, for inlet widths above 0.5 m, the rate of rise in ventilation is very limited, at 3.25%. It can be confirmed that the optimum inlet width for a solar chimney differs from a design that does not take outdoor winds into account. Due to the counterflow at the chimney outlet, previous studies [25–27] favored 0.2–0.3 m as the optimum inlet width without taking outdoor winds into account. However, after taking outdoor winds into account, the optimum inlet width is located at a relatively large 0.5 m due to the wind pressure providing additional power to the solar chimney and the relatively small backflow at the chimney outlet.

## 5. Conclusions

In this paper, a physical model of a solar chimney under the combined effect of wind pressure and thermal pressure is developed, and the natural ventilation performance of the solar chimney under different conditions of solar radiation intensity, heat flow density of the indoor heat source, outdoor wind speed, and the relative position of the indoor heat source is studied by three-dimensional numerical simulation. The main conclusions are as follows:

Within the scope of this paper, as the solar radiation intensity, indoor heat source heat flow density, and outdoor wind speed increase, their effects on the ventilation performance of solar chimney buildings are enhanced. As the intensity of solar radiation increases, solar chimney ventilation gradually increases, with a maximum increase of 33.1%. But the increase in ventilation decreases with the increase in heat flow density of the indoor heat source.

With the increase in indoor heat source heat flow density, the solar chimney ventilation volume gradually increases; the maximum value of the increase is 32.1%. The enhancement of the size of the heat source on the size of the ventilation capacity of the solar chimney

will be investigated at a later stage. When the indoor heat source is located in the middle of the room, it has a stronger influence on the effectiveness of the solar chimney draught compared to other orientations.

As outdoor wind speed increases, the amount of solar chimney ventilation also increases and increases more, but the amount of ventilation increases and decreases with the increase in solar radiation intensity and heat flow density of the indoor heat source.

Outdoor wind affects the optimum inlet width of the solar chimney, with a preference for 0.2–0.3 m as the optimum inlet width, without considering outdoor wind. However, when considering the effect of outdoor wind, the optimum inlet width is located at a relatively large 0.5 m.

**Author Contributions:** Conceptualization, S.Y. and Z.G.; methodology, S.Y., Z.G., J.X. (Jian Xu) and Z.X.; software, S.Y.; validation, S.Y. and S.Z.; formal analysis, S.Z., J.L. and J.X. (Jianbin Xie); investigation, S.Z., J.L. and J.X. (Jianbin Xie); resources, Z.X.; data curation, S.Z. and J.X. (Jian Xu); writing—original draft preparation, S.Z. and J.X. (Jian Xu); writing—review and editing, S.Y. and J.X. (Jianbin Xie) All authors have read and agreed to the published version of the manuscript.

**Funding:** This work was supported by National Natural Science Foundation of China (Grant No. 52106017), Beijing Natural Science Foundation (Grant No. 3222031), Research Fund of Yunnan Province (Grant No. 202001BB050070), Scientific Research Foundation of Kunming Metallurgy College (Grant No. Xxrcxm201802).

**Institutional Review Board Statement:** Not applicable.

**Informed Consent Statement:** Not applicable.

**Data Availability Statement:** Data are contained within the article.

**Conflicts of Interest:** The authors declare no conflict of interest.

## References

1. Tan, X.; Lai, H.; Gu, B.; Zeng, Y.; Li, H. Carbon emission and abatement potential outlook in china's building sector through 2050. *Energy Policy* **2018**, *118*, 429–439. [[CrossRef](#)]
2. Gao, X.Y.; Fan, B.Y.; Zhang, H.G. Research on the application of solar heating systems in the construction of new rural areas. *J. Sol. Energy* **2009**, *30*, 1653–1657.
3. Wang, L.; Chen, S.K.; Li, R. Study on the influencing factors and optimal design of the composite ventilation system of tunnel and solar chimney. *Renew. Energy* **2017**, *35*, 218–223.
4. Bassiouny, R.; Korah, N.S.A. Effect of solar chimney inclination angle on space flow pattern and ventilation rate. *Energy Build.* **2009**, *41*, 190–196. [[CrossRef](#)]
5. Hong, S.; He, G.; Ge, W. Annual energy performance simulation of solar chimney in a cold winter and hot summer climate. *Build. Simul.* **2019**, *12*, 847–856. [[CrossRef](#)]
6. Luo, X.L.; Wang, Y.P.; Liang, J.; Qi, J.; Su, W.; Yang, Z.; Chen, J.; Wang, C.; Chen, Y. Improved correlations for working fluid properties prediction and their application in performance evaluation of sub-critical Organic Rankine Cycle. *Energy* **2019**, *17*, 122–137. [[CrossRef](#)]
7. AboulNaga, M.M.; Abdrabboh, S.N. Improving night ventilation into low-rise buildings in hot-arid climates exploring a combined wall-roof solar chimney. *Renew. Energy* **2000**, *19*, 47–54. [[CrossRef](#)]
8. Zavala-Guillén, I.; Xamán, J.; Hernández-Pérez, I.; Hernández-López, I.; Gijón-Rivera, M.; Chávez, Y. Numerical study of the optimum width of 2a diurnal double air-channel solar chimney. *Energy* **2018**, *147*, 403–417. [[CrossRef](#)]
9. Lal, S. Experimental, CFD simulation and parametric studies on modified solar chimney for building ventilation. *Appl. Sol. Energy* **2014**, *50*, 37–43. [[CrossRef](#)]
10. Khedari, J.; Rachapradit, N.; Hirunlabh, J. Field study of performance of solar chimney with air-conditioned building. *Energy* **2003**, *28*, 1099–1114. [[CrossRef](#)]
11. Hou, Y.C.; Li, H.; Li, A.G. Experimental and theoretical study of solar chimneys in buildings with uniform wall heat flux. *Sol. Energy* **2019**, *193*, 244–252. [[CrossRef](#)]
12. Rabani, M. Cooling performance of a passive hybrid system consisted of domed roof and solar chimney: A numerical approach. *Int. J. Green Energy* **2022**, *19*, 435–454. [[CrossRef](#)]
13. Dhahri, M.; Nekoonam, S.; Hana, A.; Mamdouh, E.H.A.; Müslüm, A.; Mohsen, S.; Habib, S. Thermal performance modeling of modified absorber wall of solar chimney-shaped channels system for building ventilation. *J. Therm. Anal. Calorim.* **2021**, *145*, 1137–1149. [[CrossRef](#)]

14. He, G.Q.; Lv, D. Enhancing solar chimney ventilation efficiency by insertion of transparent panel. *J. Zhejiang Univ. Eng. Sci.* **2021**, *55*, 2260–2266.
15. Liu, H.; Li, P.; Yu, B.; Zhang, M.; Tan, Q.; Wang, Y.; Zhang, Y. Contrastive Analysis on the Ventilation Performance of a Combined Solar Chimney. *Appl. Sci.* **2022**, *12*, 156. [[CrossRef](#)]
16. Leticia, O.N.; Fernando, M.S. Simulation and measurements of wind interference on a solar chimney performance. *J. Wind. Eng. Ind. Aerodyn.* **2018**, *179*, 135–145.
17. Wang, Q.Y.; Zhang, G.M.; Li, W.Y.; Shi, L. External wind on the optimum designing parameters of a wall solar chimney in building. *Sustain. Energy Technol. Assess.* **2020**, *42*, 98–108. [[CrossRef](#)]
18. Gao, N.; Yan, Y.; Sun, R.; Lei, Y. Natural Ventilation Enhancement of a Roof Solar Chimney with Wind-Induced Channel. *Energies* **2022**, *15*, 6492. [[CrossRef](#)]
19. Shi, L. Impacts of wind on solar chimney performance in a building. *Energy* **2019**, *185*, 55–67. [[CrossRef](#)]
20. Lin, Y.; Xu, Z.Y. Buoyancy-driven flows by a heat source at different levels. *Int. J. Heat Mass Transfer.* **2013**, *58*, 312–321. [[CrossRef](#)]
21. Gao, X.P.; Li, A.G.; Yang, C.Q. Study on thermal stratification of an enclosure containing two interacting turbulent buoyant plumes of equal strength. *Build. Environ.* **2018**, *141*, 236–246. [[CrossRef](#)]
22. Barrios, G.; Huelsz, G.; Rechtman, R. Heat transfer and flow transitions of a thermal plume generated by a heating element on the enclosure bottom wall. *Eur. J. Mech. B/Fluids* **2019**, *77*, 17–24. [[CrossRef](#)]
23. Dhahri, M.; Aouinet, H.; Sammouda, H. Numerical approximation of air flow temperature distribution and thermal comfort in buildings. *Sci. Afr.* **2020**, *8*, 11–18.
24. Dhahri, M.; Aouinet, H.; Mhamdi, N. CFD analysis of the effect of uniformly sheared air flow on natural ventilation in building. *Int. J. Ambient Energy* **2019**, *43*, 915–921. [[CrossRef](#)]
25. Miyazaki, T.; Akisawa, A.; Kashiwagi, T. The effects of solar chimneys on thermal load mitigation of office buildings under the Japanese climate. *Renew. Energy.* **2006**, *31*, 987–1010. [[CrossRef](#)]
26. Arce, J.; Jimenez, M.J.; Guaman, J.D.; Heras, M.; Alvarez, G.; Xamán, J. Experimental study for natural ventilation on a solar chimney. *Renew. Energy.* **2009**, *34*, 2928–2934. [[CrossRef](#)]
27. Shi, L.; Zhang, G.M.; Yang, W.; Huang, D.; Cheng, X.; Setunge, S. Determining the influencing factors on the performance of solar chimney in buildings. *Renew. Sustain. Energy Rev.* **2018**, *88*, 223–238. [[CrossRef](#)]

**Disclaimer/Publisher’s Note:** The statements, opinions and data contained in all publications are solely those of the individual author(s) and contributor(s) and not of MDPI and/or the editor(s). MDPI and/or the editor(s) disclaim responsibility for any injury to people or property resulting from any ideas, methods, instructions or products referred to in the content.